Steady State Analysis of a Continuous Clarifier-Thickener System

Kynch's theory of sedimentation is adopted to solve for the attainable steady state concentration in a vertical continuous sedimentation basin incorporating a thickener and a clarifier. The limiting flux solution corresponding to the local minimum at the flux concentration curve is proved to have a limited range of validity and is shown to apply only to the intermediate range of feed concentrations. This limit is replaced by a five-region diagram; the solution is determined by the feed coordinates in the flux concentration plane, with respect to the flux concentration curve. Each section exhibits different characteristic solutions for both the clarifier and the thickener.

The analysis, which combines dispersion, dynamics, and stability considerations, reveals new possible ranges of operating conditions where the flux exceeds the limiting flux and solids are not entrained. The results, contradicting previous published work, are verified by a finite-difference dynamic simulator.

O. Lev, E. Rubin and M. Sheintuch
Department of Chemical Engineering
Technion-Israel Institute of Technology
Haifa 32000, Israel

SCOPE

The continuous sedimentation and clarification of solids from liquid suspensions is of special importance in an activated sludge process. This sedimentation process is susceptible to failures because of the small difference in densities between the bacteria flocs and water.

The current design and simulation methods of sedimentation basins assume, following Kynch's (1952) theory, that the gravitational component of the solids velocity is a function of solids concentration only. A limiting solid flux, corresponding to the local minimum of the flux concentration curve, is said to be the upper limit for the steady state flux transfer ability of the thickener. That was shown by Petty (1975), who solved the hyperbolic mass conservation equation for the thickener only, neglecting the end effects of the thickener and assuming no interaction between the thickener and the clarifier. Such an analysis ignores the clarifier's ability to handle the extra flux when the thickener is loaded beyond its capacity. We show that the limiting flux solution is valid only over an intermediate range of operating conditions.

Several published dynamic simulation models solve the thickener-clarifier time-dependent concentration profile. However, they are all artificially forced by extraneous means to exhibit the upper limit flux at least during steady operation. In the present work the analysis is extended to account for clarifier-thickener interaction. This analysis enables a much better and broader prediction of clarifier-thickner system behavior in steady and unsteady states of operation.

CONCLUSIONS AND SIGNIFICANCE

An original systematic analysis of clarifier-thickener interaction is presented. It incorporates Kynch's theory and takes into account the boundary conditions at the two outlets. Our analysis show three different characteristic behaviors at steady state:

1. No entrainment occurs at low solid fluxes.

Correspondence concerning this paper should be sent to M. Sheintuch.

2. The limiting flux is transferred through the thickener, while excess flux is handled by the clarifier at intermediate feed concentrations and high fluxes.

3. The feed concentration conquers the whole system when feed flux is high and feed concentration is either small or large.

These behaviors are mapped into five regions determined by the position of the feed point coordinates relative to the flux concentration curve.

A simple finite-element scheme incorporating a small Fickian dissipative term is adopted to verify the conclusions of the steady state analysis. The present scheme has a considerable advantage over existing dynamic models, since it need not impose artificial constraints to agree with steady state analysis. The scheme is simple, mathematically sound, easy to program, and can be adapted easily to deal with a multicomponent feed.

This treatment is crucial to the understanding of settler behavior during marginal operating conditions. The analysis reveals a new range of operating conditions at high concentrations which are not subjected to the limiting flux constraint. This analysis might also be valuable for experimental verification and for examining the validity of dynamic models for thickener-clarifier simulators.

Introduction

The continuous sedimentation and clarification of solids from liquid suspensions is an important unit operation in a variety of processes. Biomass thickening and effluent clarification in wastewater treatment by activated sludge have stirred a broad interest in the problem of design and operation of settlers (clarifier-thickener) under continuous steady and unsteady state operating conditions. Because of the small difference in solid (bacteria flocs) and liquid densities, this process is susceptible to failures due to shifting flow rates or changing operating conditions in the biological reactor. The latter precedes the thickener in the activated sludge process. The accurate description of the settler performance is the subject of this paper. This work is part of the broader thesis focusing on the interaction of the biological reactor and the settler (Lev, 1983).

A common assumption (due to Kynch, 1952) made in settler modeling is that the settling velocity depends only on the local solid concentration, hence neglecting inertia effects and interparticle forces (Dick, 1970; Shannon and Tory, 1966). The mass conservation condition for the thickener, the zone below the feed in Figure 1,

$$\frac{\partial C}{\partial t} = \frac{\partial J(C)}{\partial z} \tag{1}$$

can be solved by the characteristics method. The downward velocity, U, of any zone of a continuous concentration is

$$U = \left(\frac{\partial z}{\partial t}\right)_C = \left(\frac{\partial J}{\partial C}\right)_z \tag{2}$$

Now since $J(C)$ is usually nonlinear, concentration waves can propagate at different speeds and may interact to form discontinuities. Such discontinuities (wave fronts) move at a velocity of

$$U = -(J_+ - J_-)/(C_+ - C_-) \tag{3}$$

where the subscript denotes the flux or concentration values just above (+) and below (−) the discontinuity. We need to consider only stable fronts: i.e., perturbations into some continuous function across the front decay as $t \to \infty$. Lax (1973) has shown that for a front to be stable its velocity should be intermediate to the upstream and downstream velocities, i.e.,

$$(dJ/dC)_+ > (J_+ - J_-)/(C_+ - C_-) > (dJ/dC)_- \tag{4}$$

In the characteristics method this implies that characteristic lines terminate in a stable shock wave but never emanate from it.

The total flux in a continuous sedimentation is composed of batch gravitational flux and the solid convective flux

$$J = C[V_b(C) + u] \tag{5}$$

where u is positive in the downward direction. Now, since the gravitational settling velocity V_b declines with C, then $CV_b(C)$ passes through a local maximum, Figure 2. The flux concentration curve $J(C)$ admits, for sufficiently low u, a local maximum and a minimum. The minimum is denoted by (J_L, C_L).

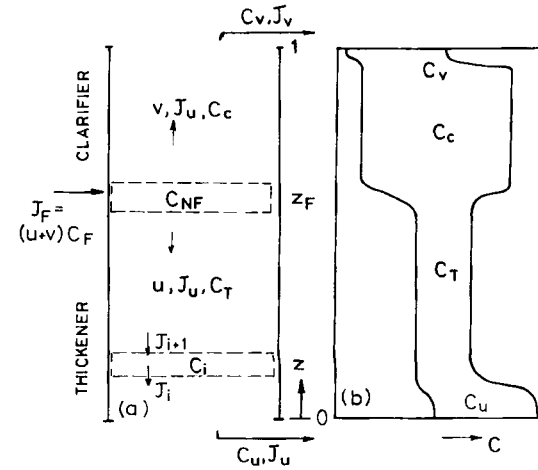

Figure 1. (a) Notation for clarifier and thickener, broken-line boxes show notation for finite-difference scheme.
(b) Attainable (monotonic) and unattainable concentration gradients.

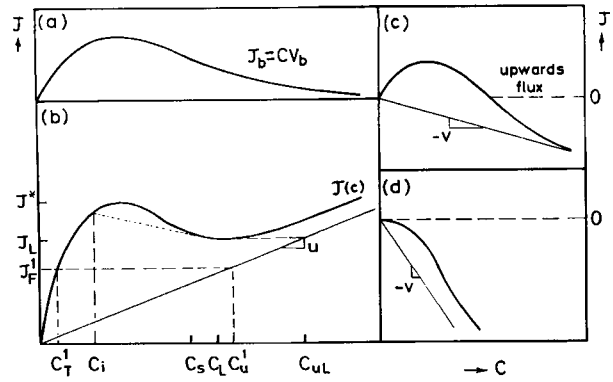

Figure 2. Characteristic flux curves in continuous sedimentation.

(a) Batch gravitational flux.
(b) Total flux in thickener
(c)(d) Total flux in clarifier for small and large entrainment velocities

The conventional theory distinguishes between two types of steady state solutions:

(a) When $J_F = J_F^1 < J_L$, there is a unique solution to Eq. 3 with $J_u = J_F^1$, the thickener concentration C_T^1 lies on the flux curve, and the underflow concentration C_u^1 lies on the convective flux line, $J_F = uC_u$.

(b) When $J^* > J_F > J_L$ the steady state equation acquires either one or three solutions when no solids entrainment into the clarifier is assumed ($J_v = 0$). Within the thickener there exists, however, a domain with $C = C_L$ which moves at a null characteristic velocity $\partial J/\partial C = 0$. That limiting concentration will eventually conquer the whole thickener, yielding a limiting flux J_L, and $C_{uL} = J_L/u$ is the underflow concentration. The balance flux $J_F - J_L$ should flow through the clarifier. This limiting flux solution applies also for $J > J^*$.

Conventional theory does not analyze the clarifier ability to handle that flux, which of course affects the settler performance. Also ignored in most analyses is the compaction zone effect that occurs at the bottom. That effect may set a limit to the underflow concentration. These steady state effects are considered in the next section and we show that steady state solutions are determined by the location of the feed point (J_F, C_F) on the map of Figure 2b.

The steady state analysis makes use of dynamic considerations; the third section is devoted to dynamic effects of the sedimentation process. Petty (1975) employed the characteristics method to describe the thickener dynamics, while neglecting clarifier effects and imposing the boundary condition that $dJ/dC > 0$ at the bottom (i.e., a sink) and at the feed (a source). One of his examples, which has commonly been employed for verification of simulation models, is that of a thickener half-filled with sediment subject to feed flux larger than the limiting one. In dimensionless concentrations and lengths, the initial and boundary conditions read

$$C(z,0) = \begin{cases} 1 & 0 \le z \le z_o \\ C_1 & z_o < z \le z_F \end{cases} \qquad C(z_F, t) = C_i \qquad (6)$$

The scales employed in the dimensionless equations are the concentration that induces zero batch velocity, the settling velocity of dilute suspensions, and the height of the sedimentation basin. The flux curve employed is $V_b(C) = (1 - C)e^{-10c}$ and $J(C_i) = J_F$. Petty's solution, shown in Figure 3a, shows negative-slope characteristic lines that correspond to $C = 0.1$ and $C = 1$ in the upper and lower part of the thickener, respectively, separated by a rarefaction wave that emanates from $(z_o, 0)$. The rarefaction wave terminates at a shock wave discontinuity that separates the initial concentration $C_+ = C_i$ and the shock wave concentration $C_- = C_s = 0.235$. The latter can be determined graphically by drawing a chord between $J(C_i)$, C_i and $J(C_s)$, C_s that is tangent at C_s (dotted line, Figure 2b). That is the graphical interpretation of Eq. 4 when $C_+ < C_-$. The limiting concentration eventually takes over the entire thickener. We will show that when the clarifier cannot handle the extra flux, $J_F - J_L$, this solution applies for short times only.

The application of the characteristics method is limited to constant or piecewise constant feed conditions, and it cannot handle time-dependent operating conditions or simulate the settler-clarifier operation when breakthrough of solids through the clarifier is not ignored. Published dynamic simulators of continuous sedimentation are based on the assumptions that there exists a limiting flux and that the clarifier is capable of handling the extra flux. This way the thickener dynamic is rendered independent of the clarifier performance.

Chi (1974) derived a dynamic model that accounts for a constant-volume mixed clarification zone that handles the extra flux, and three thickener zones corresponding to the thickening, limiting concentration, and underflow regions. The mathematical model is a finite-element representation of the characteristics method; the thickening zone is composed of layers with time-dependent volume that are removed from the system as their volume approaches zero. The layer position, height, and

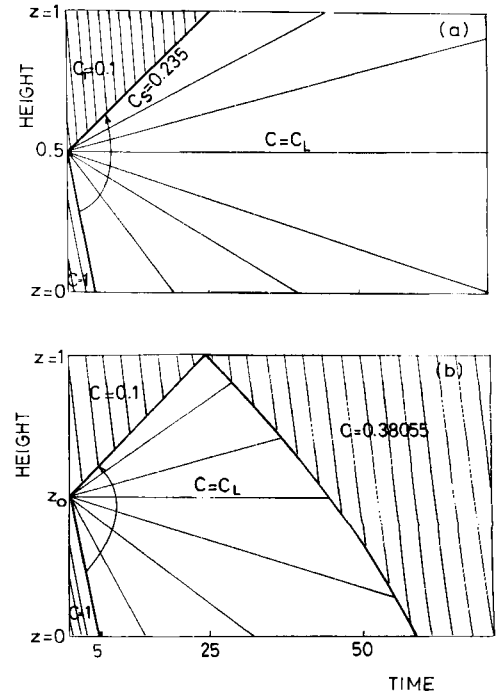

Figure 3. Solutions of problem posed by Petty (1975).

(a) Original solution (Petty, 1975)
(b) Correct solution for small v [$V_b(C) = (1 - C)e^{-10C}$, $u = 0.1$, $J_F = 0.0433$, $C_F = J_F/(u + v)$]

concentration are described by

$$\delta_i = \frac{J_{i+1} - J_i}{C_{i+1} - C_i}, \quad h_i = \delta_{i-1} - \delta_i$$

$$\frac{d(h_i C_i)}{dt} = (J_{i+1} - \delta_i C_{i+1}) - (J_i - \delta_{i-1} C_i) \tag{7}$$

Attir et al. (1977) modified the scheme to avoid an unstable shock wave: every time the above scheme violates Eq. 4 the discontinuity is replaced by a continuous concentration profile. Inverse concentration gradients are not acceptable; whenever a layer exhibits concentration larger than the one below it they are immediately mixed. Tracy and Keinath (1973) derived a forward finite-element scheme and limited the flux by setting $C = C_L$ whenever the concentration exceeds C_L.

The main drawback of schemes based on the original hyperbolic equations is the necessity of artificially imposing limiting fluxes, normal gradients, and stable discontinuities. These would be natural properties of parabolic differential equation. The inclusion of a small Fickian dispersion term in the model converts shock discontinuities into a sharp but continuous front. Anderson and Edwards (1980) incorporated such a term to account for turbulent dispersion. They still turned to an external condition for imposing a maximal limiting flux. This assumption is implicit in their finite-difference scheme.

In the third section we simulate the general clarifier-thickener problem without any artificial constraints and we show that ignoring the clarifier dynamics or imposing a limiting flux may lead to erroneous results.

Steady state analysis

The steady state solution to Eq. 1 is space- and time-independent fluxes at the thickener as well as in the clarifier. That implies a uniform concentration profile when $J_u < J_L$. When multiple solutions are possible ($J_L < J_u < J^*$), then solutions in the form of layers of different concentrations, but of identical flux, are possible. Any nonuniformity of the concentration would decay, however, upon the addition of a small dispersion term to Eq. 1. The resulting uniform concentration may not be unique and we may still find three uniform solutions when $J_L < J_u < J^*$.

In extending the analysis to the clarifier section, we assume that Kynch theory holds and the net flow is given by Eq. 5 with $(-v)$ substituted for u. This is a reasonable assumption when we restrict our attention to clarifier failure due to bulk carryover and not due to particle size distribution. Deviations from this assumption would not alter the results significantly. Qualitative analysis, however, is not then possible.

When the upward velocity v is small, solids are drawn upward ($J < 0$) only for a sufficiently large concentration, Figure 2c. For sufficiently large v, solids are entrained at any C, Figure 2d. Assuming a basin of constant cross-sectional area, uniform velocity distribution, and uniform particles, the mass balance for the clarifier can be written in the form:

$$J_F - J_u = (u + v)C_F - [u + V_b(C_T)]C_T \tag{8}$$

$$J_v = [v - V_b(C_C)]C_C = (u + v)C_C - [u - V_b(C_C)]C_C \tag{9}$$

Now, the right handside of Eq. 8 is presented graphically (arrow, Figure 4.I) by the distance between the horizontal feed

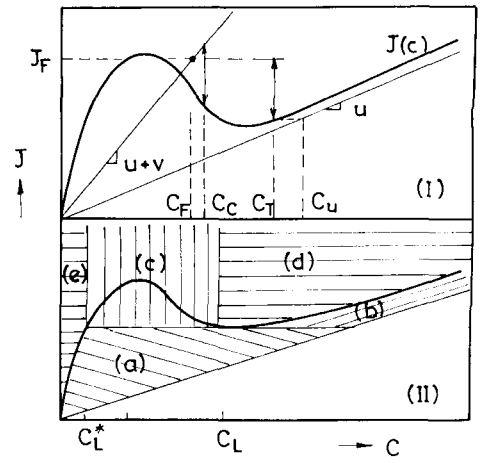

Figure 4. (I) Graphical steady state solution to clarifier-thickner problem.
(II) Domains of characteristic behavior determined by feed point location.

line; $J = J_F$, and the flux curve $J(C)$ at C_T. The rightside of Eq. 9 is the distance between the flow line, $J = (u + v)C$, and the flux curve at C_C (arrow, Figure 4I). Equation 9 may acquire an infinite number of solutions with arbitrary distribution of flux between the clarifier and the settler.

The analysis above lacks any consideration of the boundary conditions at $z = 0$ and $z = 1$. The concentration at the underflow and effluent streams are different from those in the bulk:

$$\frac{C_u}{C_T} = 1 + \frac{V_b(C_T)}{u} \qquad \frac{C_v}{C_C} = 1 - \frac{V_b(C_C)}{v} \tag{10}$$

The length required to establish the transition from C_T to C_u and from C_C to C_v, Figure 1, is assumed to be sufficiently short so that the matching of the outlet boundary layers with the settler or clarifier may be ignored. Another boundary layer exists at the feed port separating the two regions, which usually acquire different concentrations. We assume that the feed is evenly distributed so that the problem can still be described by one spatial dimension. Dispersion effects may be ignored in the bulk of the clarifier and thickener but are of importance within the boundary layers even under conditions of small solid diffusivity compared with convectional flux. These effects may eliminate certain classes of solutions.

The conservation equation, when dispersion is incorporated, reads

$$\frac{\partial C_T}{\partial t} = \frac{\partial J_T}{\partial z} + D\frac{\partial^2 C_T}{\partial z^2}, \quad \frac{\partial C_C}{\partial t} = \frac{\partial J_C}{\partial z} + D\frac{\partial^2 C_C}{\partial z^2} \tag{11}$$

and the accurate solution should satisfy these equations with appropriate boundary conditions at $z = z_F (C_C = C_T, J_F = J_C + J_T)$ and at $z = 0$ and $z = 1$. The steady state solution $C_T = C_C = C_F$ satisfies Eq. 11, the boundary condition of z_F, and the overall balance Eqs. 8–9; the two arrows in Figure 4I coalesce. This solution applies only when the feed point (C_F, J_F) lies above the flux curve $J(C)$. Thus, when dynamic factors do not prohibit, we expect the system to achieve the gradientless solution as $t \to \infty$.

The concentration profile within each section is monotonic at

steady state. If there exists a local maximum or minimum ($dC/dz = dT/dz = 0$) then from Eq. 11, $Dd^2C/dz^2 = 0$ at steady state, which cannot be satisfied for $D \neq 0$. Thus, only a negative gradient solution ($C_T > C_C$) is attainable since the solution is monotonic, Figure 1b. Inverse concentration gradients ($C_T < C_C$) are not possible as that implies the existence of extremum points in the settler and in the clarifier.

The considerations above are still insufficient for choosing the attainable solution, and we should resort to dynamic effects. Since C_L has a null characteristic velocity in the settler it will conquer the settler if $J_F > J_L$ and if the clarifier can handle the extra flux with $C_C < C_L$. Note that there are no null characteristic velocities in the clarifier. The upward flux, Figure 2c, d, is a monotonic curve of C when $J > 0$.

Five different regions of characteristic behaviors can be determined, based on the considerations above. The attainable solution, which is unique in every region, is determined from the feed point location in the (J, C) plane, Figure 4II. For specified velocities, u, v, the location of the feed point determines the flow line and feed line.

(a) When $J_F < \min [J(C_F), J_L)]$ the solution is $C_T < C_F$ and $C_C = 0$, Figure 5a. Solutions with entrainment ($J_u < J_F$) are ruled out since Eqs. 8–9 are satisfied then only with inverse concentration gradients ($C_C > C_F > C_T$). The effluent in this region, therefore, is clear of solids ($C_v = 0$).

(b) Solids entrainment through the clarifier is also ruled out in this region, with $J(C_F) > J_F > J_L$ and $C > C_L$, since it implies inverse concentration gradients. That argument eliminates also the limiting concentration solution. The settler concentration is given by $J(C_T) = J_F$; it is unique when $J_F > J^*$ and multivalued when $J_L < J_F < J^*$, Figure 5b. The intermediate solution is unstable; this can be verified by writing the mass balance on the feed zone assuming that it is well mixed and that solids are not entrained. The lower steady state $C_T = C_T^1$ satisfies the boundary conditions; yet, $C_T^1 < C_L < C_u$, and the limiting concentration that exists within the boundary layer at the bottom will eventually spread over the thickener. Now, since the clarifier cannot move any flux in this case we conclude that as $t \to \infty$ the upper state $C_T > C_L$ will eventually prevail. The limiting concentration will be washed out from the thickener by an appropriate shock wave.

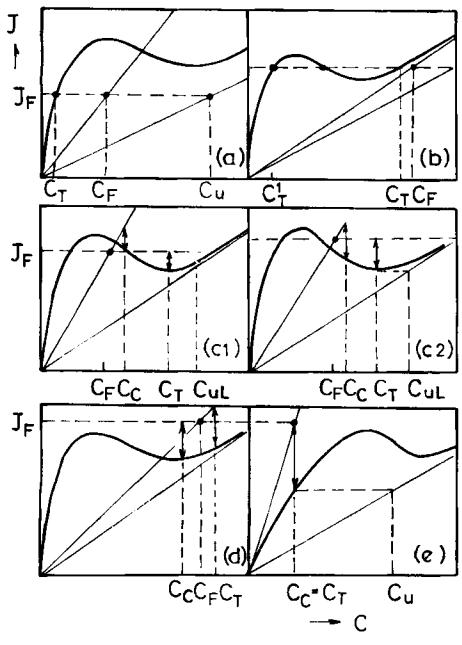

Figure 5. Characteristic steady state solutions for the five regions in Figure 4II.

(c) An infinite number of solutions is possible in this region ($J > J_L$, $C_L^* < C_F < C_L$). The limiting concentration, however, prevails as $t \to \infty$ and we can always construct the monotonic solution with

$$C_F \leq C_C \leq C_T = C_L < C_u \tag{12}$$

This conclusion holds for feed points below (Figure 5c1) or above (Figure 5c2) the flux curve.

(d) On the boundary with region (c), $C_F = C_L$ and from Eq. 12 we find that $C_F = C_T = C_C$. In region (d), where $J(C_F) > J_L$ and $C_F > C_L$, the graphical construction shows that an inverse gradient should exist to satisfy the overall balance if the limiting concentration prevails ($C_T = C_L < C_F$). If we let the limiting concentration be washed out from the settler we can still find an infinite number of monotonic solutions ($C_L < C_C < C_F < C_T$, Figure 4d). Diffusion effects will tend to eliminate any gradient across the feed boundary layer. Since the gradientless solution $C_C = C_F = C_T < C_u$ does not span the limiting concentration it will eventually persist and be stable.

(e) The relative position of the flow line and the flux line in this region, with $J(C_F) > J_F$ and $C_F < C_L^*$, is identical to that in region (d), and we conclude that the uniform solution is established at steady state Figure 5e. Note that this region incorporates points with $J_F > J_L$. The limiting flux cannot prevail under these conditions, since at any domain within the thickener where $C = C_L$, the flux is higher than that above it (J_T) and this front will propagate downward.

These conclusions are supported by dynamic simulations; several such simulations are presented in the next section.

Another basic assumption inherent to Kynch theory is the lack of any interparticle interaction so that the considerable compression effect (Eq. 8) occurring at the bottom is not bounded ($C_u \to \infty$ as $u \to 0$, Eq. 10). This compression results from the slowdown of solids from $u + V_b$ in the thickener to u in withdrawal pipes. The compression effect is bounded by the maximum possible solids concentration, C_{max}. In a batch experiment, this interpretation leads to the picture of two interfaces moving one toward the other: the lower front is the boundary of the accumulated sediment at C_{max}, and the upper front separates the bulk and initial concentrations. In a continuous system the flux through the thickener is limited either by the limiting flux or by the compression effect, which carries a maximal flux of $J_{max} = uC_{max}$, Figure 6a. Another interpretation sometimes given to C_{max} is that of the concentration of unsettling solids, i.e., $V_b(C_{max}) = 0$. In that case we always find that $J_L < J_{max}$ if $C_{max} > C_L$, Figure 6b. This interpretation, however, lacks any physical justification.

The various operating regions should be modified when J_{max} is smaller than the maximum in the flux concentration curve. When $J_{max} < J_L$ (Figure 6a) then type (a) or (e) solutions exist if $J_F < J_{max}$. When $J_F > J_{max}$ the maximal concentration spreads over the whole thickener and the excess flux should be handled by the clarifier. When $J_{max} > J_L$ then solutions of types (a)–(d) are unaffected while the gradientless solution in (e) is affected only when $J_F = J(C_F) > J_{max}$ (shaded area in Figure 6b).

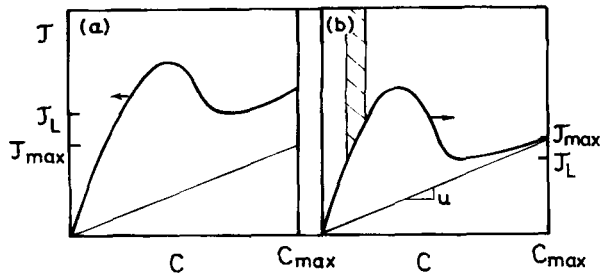

Figure 6. Steady state solution when there exists a maximal concentration.

Bifurcation diagrams

Better comprehension of the thickener-clarifier system may be gained by drawing the representative bifurcation diagrams showing the dependence of attainable solutions upon operating parameters. The parameters that can be manipulated are the total flow rate $u + v$, the underflow velocity u, and feed solids concentration C_F. We plot the characteristic diagrams with respect to C_F and with respect to underflow velocity u while maintaining all other parameters and the settling characteristics constant. Determining the dependence on $u + v$, i.e., on the solids flux, is quite straightforward.

The diagrams with C_F as the operating variable with fixed flow rates are determined by following the feed point along the flow line $J = (u + v)C$, Figure 7, upper row. We assume that as C_b increases $V_b \to 0$ so that $J(C) \to uC$ and the flow line always intercepts the flux curve $J(C)$. Three typical diagrams are shown, with the feed point spanning regions *a-b-d* for low v (Figure 7I); *a-c-d* for intermediate v (Figure 7II), and regions *e-c-d* at higher clarifier flow rates (Figure 7III). Discontinuities are observed in C_T and C_C but the underflow and overflow concentrations (C_u, C_v) are always continuous with discontinuities in the slope. These are given, in regions *a–c*, by

$$\text{(a, b)}\quad C_u = C_F\frac{u+v}{u},\quad C_v = 0,$$

$$\text{(c)}\qquad C_u = \frac{J_L}{u},\quad C_v = \frac{u+v}{v}C_F - \frac{J_L}{v} \tag{13}$$

while in regions *d–e* where the solutions are gradientless, ($C_T = C_C = C_F$)

$$\frac{C_u}{C_F} = 1 + \frac{V_b(C_F)}{u},\quad \frac{C_v}{C_F} = 1 - \frac{V_b(C_F)}{v} \tag{14}$$

Solids entrainment occurs at certain $J_F > J_L$ in diagrams I and II of Figure 7, while for sufficiently large v solids breakthrough the clarifier is already at $J_F = 0$. As C_F increases beyond the point of entrainment the separation decreases; in region *d* the underflow and effluent concentrations approach the line $C = C_F$ from above and below, respectively, since $dV_b/dC < 0$, Eq. 14.

The analysis of varying flow distribution between the clarifier and the thickener involves changing the nonlinear flux function $J(C, u)$, where u is a parameter, while keeping the feed point and flow lines unchanged. At $u = 0$, the (batch) flux curve $J(C, 0) = CV_b(C)$ passes through a local maximum while $C_L \to \infty$ and $J_L = C_L^* = 0$. For sufficiently large u, $J(C, u)$ is monotonic, Figure 8.

Other curves, with different u, can be plotted in the (J, C) plane. Since $\partial J/\partial u > 0$ these curves never intercept. The characteristic behavior is determined by the location of C_L and C_L^* defined by $J(C_L^*) = J(C_L)$ (Figure 4). The locus of these points is plotted in Figure 8 (bold lines) with u as a latent parameter. These lines coalesce and disappear at C^* where $J(C)$ acquires a zero-slope inflection point, i.e.,

$$\frac{\partial J}{\partial C}(C^*, u^*) = \frac{\partial^2 J}{\partial C^2}(C^*, u^*) = 0. \tag{15}$$

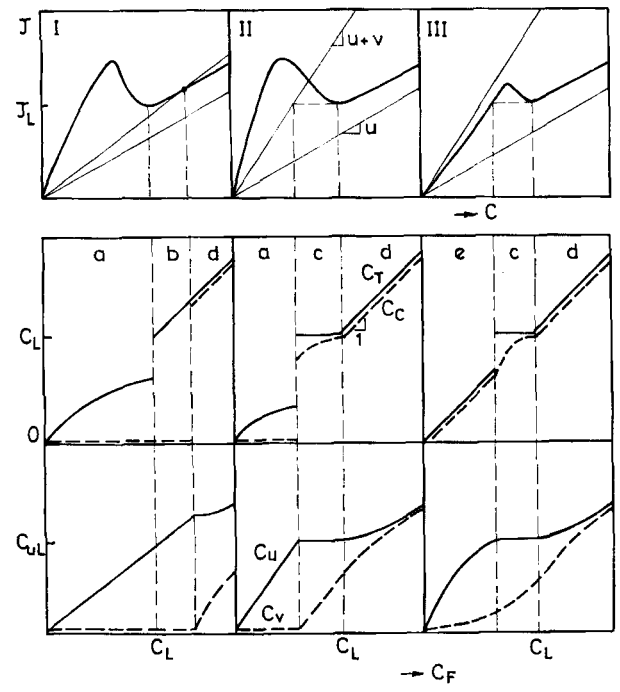

Figure 7. Bifurcation diagram with varying C_F
Top, relative positions of flux and flow line
Middle, corresponding C_T and C_C
Bottom, corresponding C_u and C_v

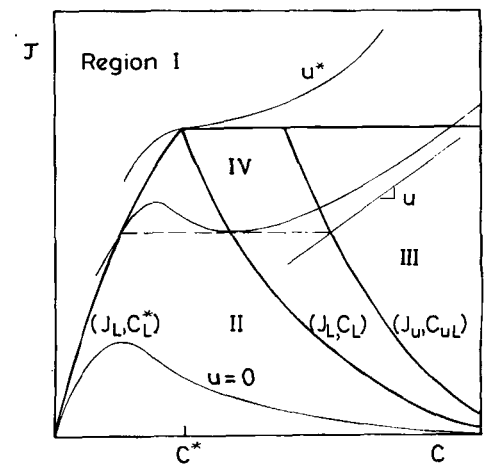

Figure 8. Domains of the four bifurcation diagrams obtained by changing ratio of thickener to clarifier flow rates.

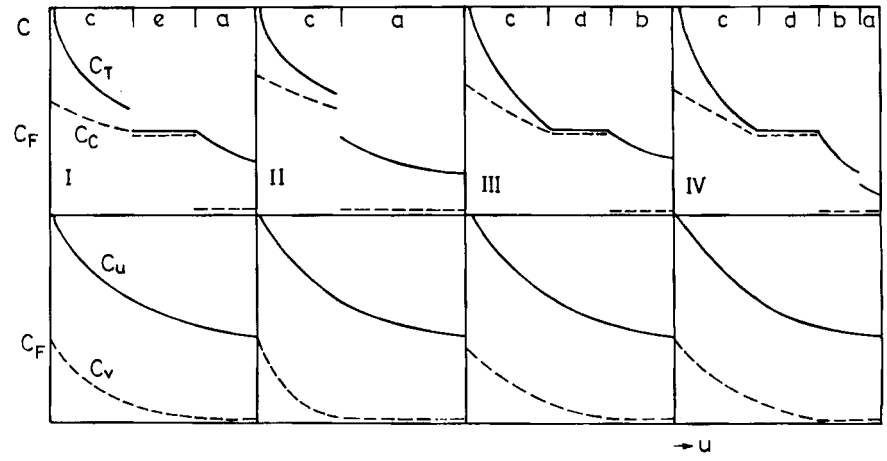

Figure 9. Bifurcation diagram with varying u; fixed $u + v$.

Also shown in Figure 8 is the locus of (J_u, C_{uL}) points and the line $J = J(C^*, u^*)$.

The bold lines in Figure 8 separate the plane into regions of different bifurcation diagrams, with respect to u. Those diagrams are shown in Figure 9. The behavior is determined by the location of the feed point (J_F, C_F), which is maintained constant. Note that as $u \to 0$ the conditions are those of a type (c) solution independent of J_F and C_F since $C_L \to \infty$ and $J(C_L)$, $J(C_L^*) \to 0$. In practice there would exist an upper concentration limit, C_{max}, but we ignore this limit in the analysis. At the other extreme as $v \to 0$ $(u \to u + v)$ the behavior is that of regions (a) or (b) in Figure 4.

The transition from solution (c) to (a) may occur directly when $J_F = J_L$ and $C_L^* < C_F < C_L$ (Figure 4), which corresponds to

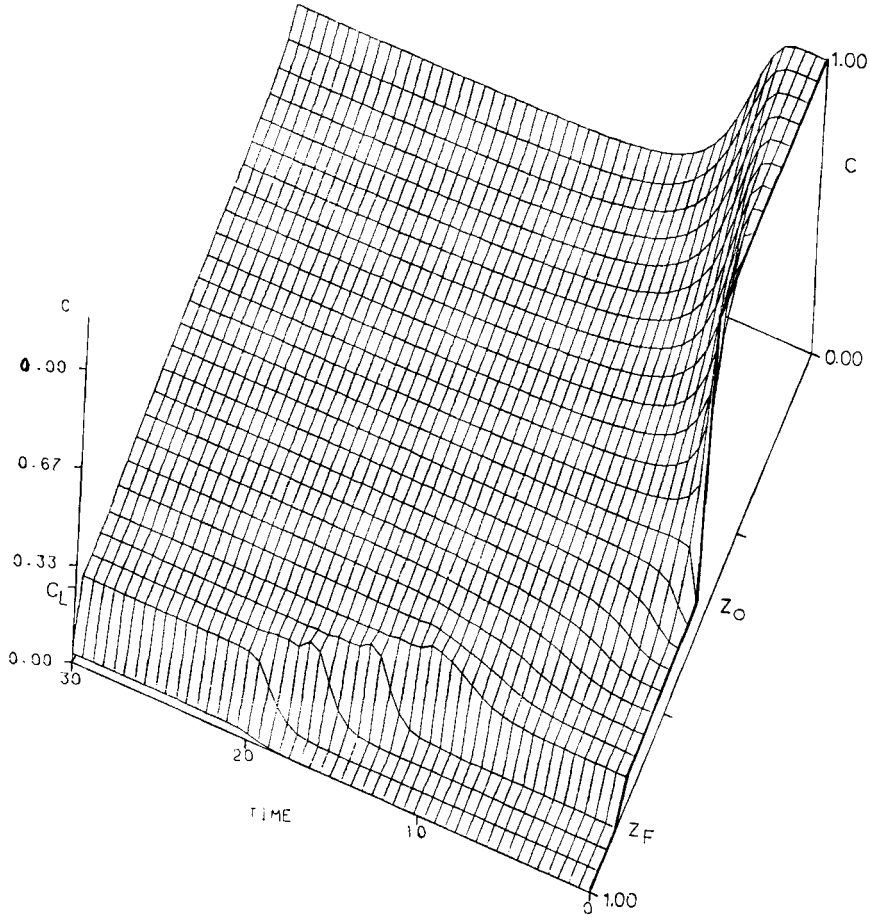

Figure 10. Breakthrough of solids from clarifier under conditions of region c in Figure 5; $v = 0.1$, all other parameters as in Figure 3.

feed points within domain II of Figure 8. If the transition occurs through a type (*e*) solution, domain I, then at the border with domain II the diagrams sweep through $(J_F, C_F) = (J_L, C_L^*)$ for a certain u. That is therefore the boundary between the two diagrams. Another path sweeps the regions *c-d-b-a* when (C_F, J_F) is in region IV. On the boundary with region I the bifurcation diagram should include the point $(J_L, C_L) = (J_F, C_F)$ for some u. When $J_F > J_L$ for any $u < u + v$ (region IV) the system remains in region *b* as $v \to 0$.

The underflow and overflow concentrations decline monotonically with u. The optimal operating position is just at the boundary of region *a*, where C_u is maximal within the region and entrainment through the clarifier does not occur yet.

The importance of drawing these diagrams lies in their instructive values for operational purposes of commercial units. These diagrams may also be verified experimentally and the location of the discontinuities will then provide crucial information concerning the validity of the batch sedimentation experiments for design of continuous operation. Note that the discontinuities are evident in the measurement of C_T, C_C but may be difficult to detect when C_u and C_v are measured.

Dynamic simulation

In deriving the dynamic model we assume uniformity of cross-sectional area and of radial fluid velocity, and incompressible solids with gravitational velocity that is dependent on C only. We include a small Fickian dispersion term to write the model in the form of Eq. 11. The corresponding finite-difference scheme is in the form (see notation in Figure 1):

$$\frac{dC_i}{dt} = \frac{J_{i+1} - J_i}{\Delta z} + \frac{D}{\Delta z^2}(C_{i+1} - 2C_i + C_{i-1}) \tag{16}$$

$$J_i = \begin{cases} (u + V_b)C_i, & z < z_F, i < NF \\ (-v + V_b)C_i, & z > z_F, i > NF \end{cases} \tag{17}$$

This scheme was solved in the direction of flow in each region. Continuity of concentration and discontinuity of fluxes at the feed was satisfied by writing an overall mass balance on the feed cell

$$\frac{dC_{NF}}{dt} = (u + v)C_F - \{[(u + V_b(C_{NF})] - [(v - V_b(C_{NF})]\} C_{NF} + \frac{D}{\Delta z^2}(C_{NF+1} - 2C_{NF} + C_{NF-1}) \tag{18}$$

The terms on the righthand side account for the feed, flux to the thickener, flux to the clarifier, and dispersion. The flux upward is set to 0 when $v - V_b(C_{NF}) < 0$. The boundary conditions at $z = 0$ and $z = 1$ were taken to be

$$J_1 = J(t, 0) = uC_1, \quad J_{N+1} = J(t, 1) = vC_N \tag{19}$$

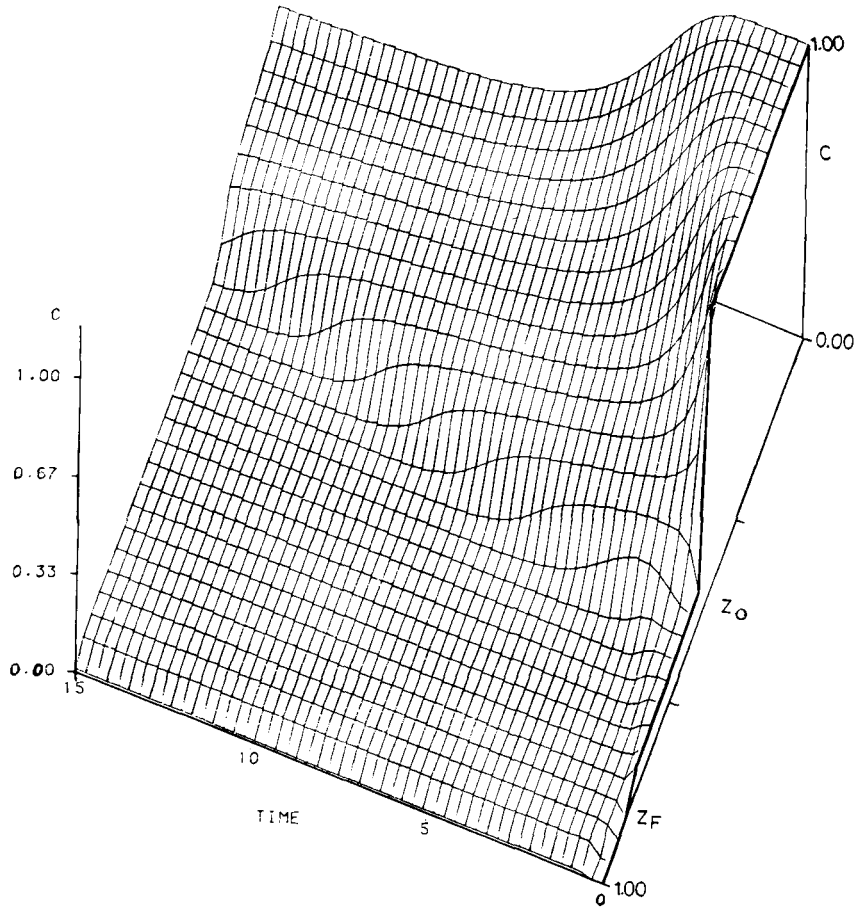

Figure 11. Establishment of gradientless solution under conditions of region *e* in Figure 5; $v = 0.8$, all other parameters as in Figure 3.

The dispersion term satisfies $D/uZ \ll 1$ so that it is of importance only when sharp gradients exist. When maximal compression concentration C_{max} was imposed, we set $J_{i+1} = uC_{max}$ if C_i exceeds C_{max}; this causes a solid accumulation effect.

To demonstrate the dynamics of clarifier-thickener systems we have solved Petty's example number 2 for various values of v while maintaining $C_F = 0.1$, $J_F = 0.0433$, and $J(C) = C(1 - C)e^{-10C}$. The clarifier $(0.84 < z < 1)$ is initially free of solids while in the thickener the distribution is like that in the original problem. Note that the concentration of $C(z_F, t)$ does not have to be specified.

When $v = 0$, the parameters fall within region b of Figure 5. Steady state analysis shows that when the feed point is within that region there is no entrainment. Yet the thickener concentration is not C_L, as suggested in the original solution, but the upper solution of $J(C_T) = J_F$. We present the dynamic solution for the case of no entrainment ($v = 0$) by the method of characteristics, Figure 3b. Our solution is in agreement with the original solution until the shock wave rising from z_o reaches the feed port, at $t = 24.8$. Then the domain of lower steady state solution disappears from the thickener. The concentration in the feed zone must jump, therefore, to the upper solution of $J(C|_{z=z_F}) = J_F$. Then a downward shock between $C_T = C_+ = 0.38$ and varying C_- is reflected downward. The velocity of this front, Eq. 3, varies with z and the shock characteristic is concave. This result was verified by a finite-scheme simulation.

At higher upward velocities, Figure 10, $v = 0.1$, breakthrough occurs after the shock wave reaches the feed port. The long-time solution corresponds to that of region c, $C_T = C_L$ and $C_C > C_F$. At high upward velocities that correspond to region e, solids break through the clarifier immediately, establishing a low concentration there. A front separating that concentration and the limiting concentration at the bottom moves downward with time. Eventually the gradientless solution will be established, Figure 11. For conditions of large flux and concentrations (region d) the thickener fails and the feed concentration spreads over both sections, Figure 12.

The above scheme can also be used to model the settling of a heterogeneous feed composed of nonuniform particle sizes or of various solid species. The overall flux from any layer is the sum of all flux corresponding to the different populations within the layer. Denote X_j as the partial concentration of population j, i.e., $C = \Sigma X_j$. If batch sedimentation velocity is determined by C, we may write

$$J_j = X_j[u + V_b(C)] \tag{20}$$

The dynamic model accounts then for the balance of each species.

Concluding Remarks

A sedimentation basin should be designed to operate in region a or b of Figure 5 where solids do not break through the clarifier.

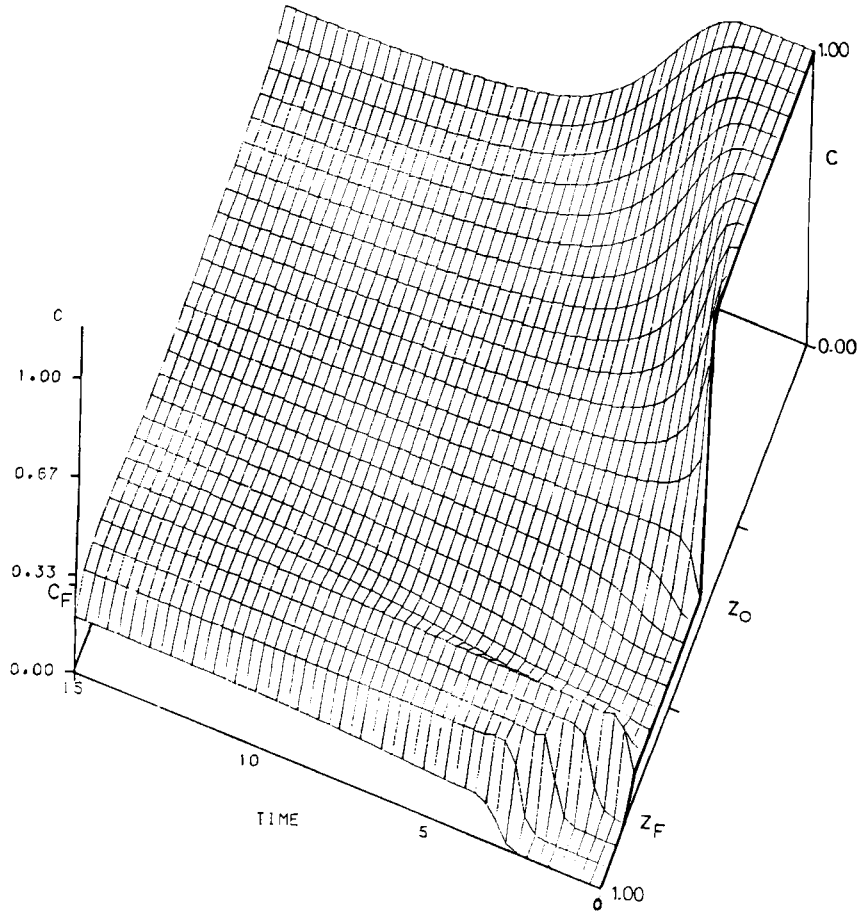

Figure 12. Establishment of a gradientless solution under conditions of region d in Figure 5; $J_F = 0.06$, $C_F = 0.3$, all other parameters as in Figure 3.

To increase output the thickener fluid velocity v should be as close as possible to the boundary with regions c or d with a certain safety margin to avoid failures due to perturbations. Any control scheme should be based on the signal of the clarifier concentration C_C, which is more sensitive and of faster response than the overflow solids concentration C_V, as is evident from Figure 9. Moreover our analysis shows that such control is superior to the so-called blanket control, which employs C_T as a signal and adjusts the flow to arrest the rise of the high-concentration shocks. The blanket control excludes operation in region b, which can be realized only after the high-concentration shock front reaches the feed zone and leaves the system (Figure 3b). Operation in region b is the optimal operating condition for high feed concentrations since the underflow flux is larger than the limiting one and solids do not break through the clarifier. This region may be too small, however, to allow for safe operation without proper control.

The main reason for failures in the activated sludge process is not surges in the feed concentration and fluxes, but changes in the settling properties, i.e., in the parameters that determine $V_b(C)$. The literature suggests several factors that affect the flocculation process and hence the settling velocity. The main ones are the concentration of polysaccharide—an exocellular polymer that serves as a flocculant—and the existence of filamentous growth that prevents sedimentation. These are the mediators of the interaction between the reactor and the thickener design. We are currently studying the effect of the reactor operating conditions on the production of exocellular polymer and filamentous growth and their subsequent impact on sedimentation. Once these effects are quantified, a combined model of the reactor and sedimentation basin may be employed for design and optimization purposes.

Acknowledgment

This research was supported by a grant from the National Council for Research and Development, Israel, and the KFK-Karlsruhe, Germany.

Notation

C = solids concentration
C_L^* = lower concentration corresponding to J_L
D = dispersion coefficient
h = height of discrete layer
J = solids flux
N = number of finite-difference elements
NF = number of the feed point element
t = time
U = waves velocity
u = thickener fluid velocity
V_b = solids batch settling velocity
v = clarifier fluid velocity
X = partial concentration
Z = settler height
z = length coordinate
δ = layer interface velocity

Subscripts

C = clarifier
F = feed
NF = at feed location
L = limiting
max = at the maximum concentration
T = thickener
u = underflow
U_L = underflow corresponding to limit
v = overflow
+, − = upstream, downstream shock properties

Literature Cited

Anderson, H. M., and R. V. Edwards, "A Finite-Differencing Scheme for the Dynamic Simulation of Continuous Sedimentation," *AIChE Symp. Ser., Water,* **77,** 227 (1980).

Attir, U., M. M. Denn, and C. A. Petty, "Dynamic Simulation of Continuous Sedimentation," *AIChE Symp. Ser.,* **73,** 49 (1977).

Chi, J., "Optimal Control Policies for the Activated Sludge Processes," Ph.D. Diss. State Univ. New York, Buffalo (1974).

Dick, R. I. "Role of Activated Sludge. Final Settling Tanks," *J. San. Eng. Div. ASCE,* **96,** 423 (1970).

Kynch, G. J. "A Theory of Sedimentation," *Trans. Faraday Soc.,* **48,** 166 (1952).

Lax, P. D., "Hyperbolic systems of Conservation Laws and the Mathematical Theory of Shock Waves," *Regional Conf. Ser.* in *Appl. Math* No. 11SIAM, Philadelphia (1973).

Lev, O., "A Dynamic Model for an Activated Sludge Reaction and Settler," (in Hebrew) M.Sc. Thesis, Technion IIT, Israel (1983).

Petty, C.A., "Continuous Sedimentation of a Suspension with a Nonconvex Flux Law," *Chem. Eng. Sci.,* **30,** 1,451 (1975).

Shannon, P. T., and E. M. Tory, "The Analysis of Continuous Thickening," *AIME Trans.,* **237,** 375 (1966).

Tracy, K. D., and T. M. Keinath, "Dynamic Model for Thickening of Activated Sludge," *AIChE Symp. Ser., Water,* **70,** 291 (1973).

Manuscript received Dec. 10, 1984, and revision received July 10, 1985.